

Wideband Beam Tracking Based on Beam Zooming for THz Massive MIMO

Jingbo Tan and Linglong Dai

Beijing National Research Center for Information Science and Technology,

Department of Electronic Engineering,

Tsinghua University, Beijing 100084, China

E-mail: tanjb17@mails.tsinghua.edu.cn, dail@tsinghua.edu.cn

Abstract—Terahertz (THz) multiple-input multiple-output (MIMO) is becoming a promising technology for future 6G network, where using beam tracking scheme to track mobile users is essential. However, existing beam tracking schemes designed for narrowband systems with the traditional hybrid precoding structure suffer from severe performance loss caused by the wideband beam split effect. To solve this problem, we propose a beam zooming based beam tracking scheme by considering the recently proposed delay-phase precoding structure. At first, we prove the beam zooming mechanism to flexibly control the angular coverage of frequency-dependent beams over the whole bandwidth, i.e., the degree of the wideband beam split effect, which is achieved by the elaborate design of time delays in the delay-phase precoding structure. Based on this mechanism, we then propose to track multiple physical directions in each time slot by generating multiple beams. The angular coverage of these beams are flexibly zoomed to match the angular variation range of user physical direction. After several time slots, the base station can obtain the new physical direction by finding out the beam with the largest received power. The proposed scheme can track multiple physical directions simultaneously with reduced training overhead, which is verified by simulation results.

Index Terms—THz massive MIMO, beam tracking.

I. INTRODUCTION

Terahertz (THz) massive multiple-input multiple-output (MIMO) is considered as a promising technology for future 6G network [1]. It can provide tenfold more bandwidth, and compensate for the severe path loss through high-array-gain beams. Nevertheless, traditional hybrid precoding structure in massive MIMO cannot deal with the beam split effect caused by the vary large bandwidth and a very large number of antennas [2], [3]. Specifically, the beam split effect means the beams generated by the traditional *frequency-independent* phase-shifters (PSs) may split into different physical directions over different subcarriers within the large bandwidth, which results in a serious array gain loss and thus an achievable sum-rate loss. To solve this problem, we have proposed the delay-phase precoding structure by introducing a time delay network as a new precoding layer, which can mitigate the array gain loss caused by the beam split effect [3].

Considering that the THz channel is quasi-optical with a single dominant path [4], the beam selection based hybrid precoding method, which chooses the beam with the highest array gain for each user, is able to achieve the near-optimal achievable sum-rate [5]. To realize the beam selection, the channel information is essential. However, it is difficult for the base station (BS) to obtain the accurate channel information of large size in THz massive MIMO systems. More seriously,

due to the narrow width of high-array-gain beams, the optimal beam varies fast due to the user mobility. Hence, traditional channel estimation schemes will result in high training overhead in THz massive MIMO systems [6]. To avoid such high training overhead, the efficient beam tracking schemes are more practical for THz massive MIMO systems [7]–[9].

The existing beam tracking schemes mainly utilize a training procedure between the BS and the user to find the optimal beam from a beam codebook [7]–[9]. For instance, [7] searched the optimal beam from a beam codebook containing potential beams through a single-sided exhausted training procedure. To reduce the unacceptable training overhead caused by the large codebook size, an adaptive search scheme was proposed by using the hierarchical codebook [8]. In addition, an auxiliary beam pair based beam tracking scheme was proposed, where the optimal beam was obtained based on the user received signals of two auxiliary beams generated by two extra RF chains [9]. Unfortunately, although the current beam tracking schemes can achieve acceptable performance, they are mainly designed for narrowband systems with traditional hybrid precoding structure [7]–[9]. In wideband THz massive MIMO systems, these schemes may suffer from severe performance degradation due to the beam split effect. To the best of our knowledge, this wideband beam tracking problem for THz massive MIMO has not been addressed in the literature.

To fill in this gap, we propose a beam zooming based beam tracking scheme by using the delay-phase precoding structure [3]. Specifically, we first reveal the beam zooming mechanism to control the angular coverage of frequency-dependent beams generated by the delay-phase precoding structure. Then, based on this mechanism, we propose to track multiple physical directions through multiple frequency-dependent beams simultaneously in each time slot. The angular coverage of these beams can be flexibly controlled to cover a fraction of the angular variation range of user physical direction. After several time slots, the BS can obtain the optimal beam based on the user received signal power. Unlike traditional beam tracking schemes which usually track only one physical direction in each time slot, the proposed scheme is able to track multiple physical directions in each time slot. Thus, it can realize accurate beam tracking with significantly reduced training overhead, which is verified by simulation results¹.

¹The simulation codes are provided to reproduce the results in this paper at <http://oa.ee.tsinghua.edu.cn/dailinglong/publications/publications.html>.

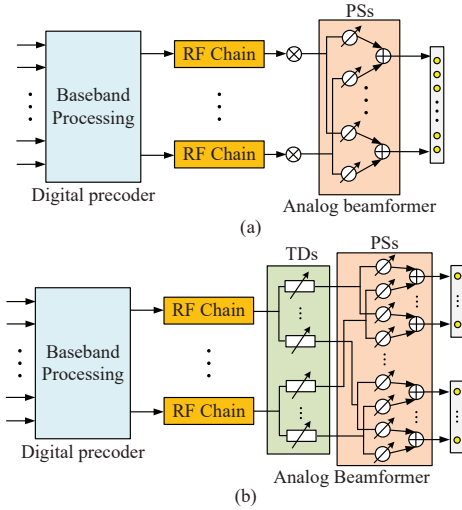


Fig. 1. (a) Traditional hybrid precoding structure; (b) DPP structure.

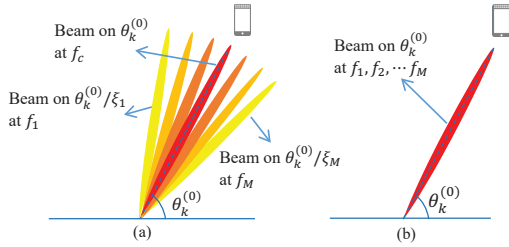


Fig. 2. (a) Beam split effect; (b) Beams generated by the DPP structure.

II. SYSTEM MODEL

We consider a multi-user wideband THz massive MIMO system. The BS employs an N -antenna uniform linear array to serve K single-antenna users, where OFDM with M subcarriers is used over the bandwidth B .

A. Channel Model

We consider the widely used ray-based channel model for the wideband THz channel [10]. The channel $\mathbf{h}_{k,m} \in \mathcal{C}^{N \times 1}$ of user k at subcarrier m is denoted as

$$\mathbf{h}_{k,m} = \sum_{l=0}^{L-1} \beta_{k,m}^{(l)} \mathbf{a}_N(\psi_{k,m}^{(l)}), \quad (1)$$

where $\beta_{k,m}^{(l)} = g_{k,m}^{(l)} e^{-j\pi\tau_{k,m}^{(l)} f_m}$ with $g_{k,m}^{(l)}$, $\tau_{k,m}^{(l)}$ denoting the path gain and the time delay of the l -th path, f_m is the frequency of subcarrier m satisfying $f_m = f_c + \frac{B}{M}(m-1 - \frac{M-1}{2})$ with f_c being the carrier frequency, L is the number of paths, $\psi_{k,m}^{(l)}$ is the l -th path spatial direction of the k -th user at subcarrier m . $\mathbf{a}_N(\psi_{k,m}^{(l)})$ denotes the array response as $\mathbf{a}_N(\psi_{k,m}^{(l)}) = (1/\sqrt{N})e^{j\pi\psi_{k,m}^{(l)}\mathbf{p}(N)}$ with $\mathbf{p}(N) = [0, 1, \dots, N-1]^T$. The spatial directions are defined as $\psi_{k,m}^{(l)} = \frac{2d}{c} f_m \sin \tilde{\theta}_k^{(l)}$, where $\tilde{\theta}_k^{(l)}$ denotes the physical direction of the l -th path, $d = \frac{f_c}{2c}$ is the antenna spacing with c being the light speed. For simplification, we use $\theta_k^{(l)} = \sin \tilde{\theta}_k^{(l)} \in [-1, 1]$ in this paper.

Due to the severe path loss, THz communications rely on the line-of-sight (LoS) path [4], which makes beam selection schemes near-optimal [5]. In the beam selection, each user is served through a beam, which is aligned with the physical

direction of the LoS path $\theta_k^{(0)}$ (we denote the path with $l=0$ as the LoS path). Hence, when traditional hybrid precoding structure as shown in Fig. 1 (a) is applied at the BS [2], the beam \mathbf{f}_k for the k -th user generated by traditional frequency-independent PSs, is usually set as $\mathbf{f}_k = \mathbf{a}_N(\theta_k^{(0)})$ [5]. However, in wideband THz massive MIMO, the frequency-independent beam \mathbf{f}_k may split into different physical directions because of the ultra-wide bandwidth and large number of antennas. This effect is called beam split effect. Specifically, as proved by **Lemma 1** in [3], the beam \mathbf{f}_k will be aligned with the physical direction $\theta_{k,m}$ at subcarrier m as

$$\theta_{k,m} = (f_c/f_m) \theta_k^{(0)} = \theta_k^{(0)}/\xi_m, \quad (2)$$

where $\xi_m = \frac{f_m}{f_c}$. It is clear from (2) that \mathbf{f}_k may point to frequency-dependent physical directions at different subcarriers. Therefore, as shown in Fig. 2 (a), when we consider the ultra-wide bandwidth and very narrow beam caused by the large number of antennas, the beam \mathbf{f}_k cannot be aligned with the target user in a certain direction at most subcarriers. As a result, traditional hybrid precoding structure will suffer from a severe achievable sum-rate loss [3].

B. Delay-Phase Precoding

To cope with the performance loss caused by the beam split effect, we consider the recently proposed delay-phase precoding (DPP) structure at the BS as shown in Fig. 1 (b) [3]. In DPP structure, a time delay network is introduced between RF chains and PS network. Specifically, each RF chain connects K_d time-delayers (TDs), and the K_d TDs connect to all the antenna elements in a sub-connected manner, i.e., each TD connects to P antenna elements through traditional PSs where $P = \frac{N}{K_d}$ is assumed to be an integer. We further assume the number of RF chains $N_{\text{RF}} = K$. Thus, the received signal $\mathbf{y}_m \in \mathcal{C}^{K \times 1}$ for K users at subcarrier m is

$$\mathbf{y}_m = \mathbf{H}_m^H \mathbf{A}_m \mathbf{D}_m \mathbf{s} + \mathbf{n}, \quad (3)$$

where $\mathbf{H}_m = [\mathbf{h}_{1,m}, \mathbf{h}_{2,m}, \dots, \mathbf{h}_{K,m}]$ denotes the channel matrix between the BS and K users at subcarrier m , $\mathbf{A}_m \in \mathcal{C}^{N \times K}$ denotes the analog beamformer realized by frequency-independent PSs and TDs, $\mathbf{D}_m \in \mathcal{C}^{K \times K}$ is the digital precoder satisfying the transmit power constraint $\|\mathbf{A}_m \mathbf{D}_m\|_F \leq \rho$ with ρ being the transmission power per user, and \mathbf{n} is noise vector satisfying Gaussian distribution $\mathcal{CN}(0, \sigma^2 \mathbf{I}_K)$ with σ presenting the noise power. By introducing TDs, the analog beamformer is composed of two parts as $\mathbf{A}_m = \mathbf{A}^s \mathbf{A}_m^d$. On one hand, $\mathbf{A}^s = [\mathbf{A}_1^s, \mathbf{A}_2^s, \dots, \mathbf{A}_K^s]$ is realized by traditional PSs, where $\mathbf{A}_k^s \in \mathcal{C}^{N \times K_d} = \text{diag}([\mathbf{a}_{k,1}, \mathbf{a}_{k,2}, \dots, \mathbf{a}_{k,K_d}])$ with $\mathbf{a}_{i,j}$ denoting the beamforming vector provided by the P PSs connected to the j -th TD corresponding to the i -th RF chain, with restriction $|\mathbf{a}_{i,j,[p,q]}| = \frac{1}{\sqrt{N}}$ [11]. On the other hand, \mathbf{A}_m^d has the form

$$\mathbf{A}_m^d = \text{diag}([e^{-j2\pi f_m \mathbf{t}_1}, e^{-j2\pi f_m \mathbf{t}_2}, \dots, e^{-j2\pi f_m \mathbf{t}_K}]), \quad (4)$$

which is realized by TDs, where $\mathbf{t}_i \in \mathcal{C}^{K_d \times 1}$ is the time delays provided by the K_d TDs that connected to the i -th RF chain.

We can observe from (4) that TDs can realize frequency-dependent phase shifts. Therefore, the DPP structure converts traditional frequency-independent beamforming into frequency-dependent beamforming. [3] has proved the principle to generate beams aligned with each user at all subcarriers with a near-optimal array gain in the DPP structure, as shown in Fig. 2 (b). Specifically, denoting $\mathbf{f}_{k,m} = \mathbf{A}_k^s e^{-j2\pi f_m \mathbf{t}_k}$ as the frequency-dependent beam for the k -th user at subcarrier m which satisfies $\mathbf{A}_m = [\mathbf{f}_{1,m}, \mathbf{f}_{2,m}, \dots, \mathbf{f}_{K,m}]$, \mathbf{A}_k^s and \mathbf{t}_k should follow the form as

$$\mathbf{A}_k^s = \text{diag}\left(\underbrace{[\mathbf{a}_P(\theta_k^{(0)}), \mathbf{a}_P(\theta_k^{(0)}), \dots, \mathbf{a}_P(\theta_k^{(0)})]}_{K_d \text{ columns}}\right), \quad (5)$$

$$\mathbf{t}_k = s_k T_c \mathbf{p}(K_d), \quad s_k = -\left(P\theta_k^{(0)}\right)/2, \quad (6)$$

where $T_c = \frac{1}{f_c}$ is the period of the carrier frequency, and s_k denotes the number of periods that delayed by TDs. Based on (5) and (6), the severe performance loss caused by the beam split effect can be eliminated, which makes DPP structure promising for wideband THz massive MIMO systems [3].

C. Frame Structure for THz Beam Tracking

We consider a widely used frame structure as shown in Fig. 3 for beam tracking [8]. Firstly, the full channel estimation is carried out at the beginning of each block. Then, in a block, the physical direction of LoS path varies in a much smaller time scale, which is defined as a frame. Within a frame, the beam tracking scheme is carried out first, where new physical directions are tracked. Based on new physical directions, the analog beamformer \mathbf{A}_m can be determined to generate directional beams according to (5), (6). Thus, the received signal converts to $\mathbf{y}_m = \mathbf{H}_{m,\text{eq}}^H \mathbf{D}_m \mathbf{s} + \mathbf{n}$, where $\mathbf{H}_{m,\text{eq}}^H = \mathbf{H}_m^H \mathbf{A}_m$ is the low-dimensional equivalent channel, which can be easily estimated using traditional channel estimation methods with a low training overhead. After that, the digital precoder \mathbf{D}_m can be determined based on $\mathbf{H}_{m,\text{eq}}$, and finally the data can be transmitted using \mathbf{A}_m and \mathbf{D}_m for hybrid precoding.

In the above frame structure, the accuracy of beam tracking scheme has a crucial impact on the achievable sum-rate. Unfortunately, the traditional beam tracking schemes [7]–[9], which are designed for narrowband systems with traditional hybrid precoding structure, cannot deal with the beam split effect, which induces serious achievable sum-rate loss. Therefore, a more efficient beam tracking scheme is preferred for wideband THz massive MIMO systems.

III. THE PROPOSED FLEXIBLE BEAM ZOOMING BASED BEAM TRACKING SCHEME

In this section, we first discuss the direct application of traditional beam tracking scheme [7] for the DPP structure. Then, we prove the beam zooming (BZ) mechanism to flexibly control the angular coverage of beams, based on which a BZ based beam tracking scheme is proposed.

A. Traditional Beam Tracking Scheme Using DPP

To avoid the severe performance loss incurred by the beam split effect, it is intuitive to apply traditional schemes for the

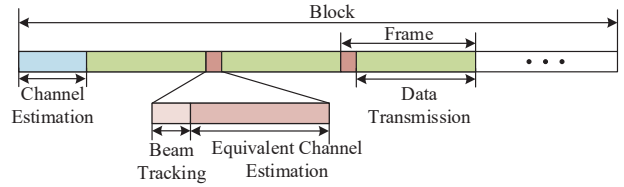


Fig. 3. The frame structure for THz beam tracking.

DPP structure. Therefore, we first discuss the direct application of one typical traditional scheme [7] for the DPP structure, which can serve as the benchmark for comparison.

Denote the physical directions of user k at the i -th frame as $\theta_{k,i}^{(0)}$, the target of beam tracking is to track $\theta_{k,i+1}^{(0)}$ based on $\theta_{k,i}^{(0)}$. In this paper, we assume a simple prior information that the BS knows the potential motion range of the users physical directions α_k , which means $\theta_{k,i+1}^{(0)}$ lies in a tracking range as $[\theta_{k,i}^{(0)} - \alpha_k, \theta_{k,i}^{(0)} + \alpha_k]$. This variation range α_k can be obtained through efficient user trajectory prediction in advance [12].

In the traditional scheme [7], single physical direction is tracked in each time slot until the tracking range is traversed, using T time slots in total. Specifically, at the t -th time slot with $t = 1, 2, \dots, T$, beams $\mathbf{f}_{k,m}$ aligned with the physical direction $\bar{\theta}_{k,i}^{(t)}$ over the whole bandwidth are generated by the DPP structure for the k -th user according to (5) and (6) with

$$\bar{\theta}_{k,i}^{(t)} = \theta_{k,i}^{(0)} - \alpha_k + (2t - 1) \frac{\alpha_k}{T}. \quad (7)$$

In this way, $\bar{\theta}_{k,i}^{(t)}$ with $t = 1, 2, \dots, T$ can uniformly cover the tracking range $[\theta_{k,i}^{(0)} - \alpha_k, \theta_{k,i}^{(0)} + \alpha_k]$. Then, the BS transmits pilot sequence to the user during each time slot. After T time slots, the optimal beam for the next frame with the largest received power can be selected out and fed back from the user to the BS.

The traditional beam tracking scheme using DPP structure can realize beam tracking without severe performance loss caused by the beam split effect. Nevertheless, due to the narrow beam width in THz massive MIMO, to achieve sufficient tracking accuracy of the physical direction, the required training overhead T is too large, e.g., when $N = 256$ and $\alpha_k = 0.1$, T should be larger than 52, which is unacceptable in practice. Therefore, the solution to the low overhead beam tracking is vital for wideband THz massive MIMO systems.

B. Beam Zooming Mechanism

The reason for high training overhead of the traditional beam tracking scheme is that, only one physical direction can be tracked during a single time slot. This problem cannot be easily solved in traditional hybrid precoding structure, since only one frequency-independent beam can be generated using traditional PSs for one RF chain over the whole bandwidth. In contrast, by utilizing time delays, the DPP structure can flexibly control the angular coverage of generated frequency-dependent beams. If the beams at different subcarriers are aligned with different physical directions and cover the tracking range, multiple physical directions can be tracked simultaneously. As a result, a low training overhead can be expected.

Inspired by this idea, we reveal the BZ mechanism to control the angular coverage of beams generated by the DPP structure in **Lemma 1**, where the frame index i is ignored.

Lemma 1. Consider the k -th user and denote $\phi_k = \theta_k^{(0)} + (1 - \xi_1)\alpha_k$. When the number of periods that delayed by TDs $s_k = -\frac{P}{2}(\phi_k + \frac{2\xi_M\xi_1\alpha_k}{\xi_M - \xi_1})$, the beams for the k -th user at the m -th subcarrier $\mathbf{f}_{k,m}$ which satisfies $\mathbf{f}_{k,m} = \mathbf{A}_k^s e^{-j2\pi f_m \mathbf{t}_k}$, where $\mathbf{A}_k^s = \text{diag}(\mathbf{a}_P(\phi_k) e^{j\pi(P\phi_k + 2s_k)\mathbf{p}(K_d)})$ and $\mathbf{t}_k = s_k T_c \mathbf{p}(K_d)$, is aligned with the physical direction $\bar{\theta}_{k,m}$ as

$$\bar{\theta}_{k,m} = \theta_k^{(0)} + (1 - \xi_1)\alpha_k + \frac{2\xi_M\xi_1(\xi_m - 1)}{\xi_m(\xi_M - \xi_1)}\alpha_k. \quad (8)$$

Moreover, $\bar{\theta}_{k,m}$ with $m = 1, 2, \dots, M$ can cover the tracking range $[\theta_k^{(0)} - \alpha_k, \theta_k^{(0)} + \alpha_k]$.

Proof: To prove **Lemma 1**, we first list a useful lemma which describes how the DPP structure adjusts the physical direction of the frequency-dependent beams.

Lemma 2. When $\bar{\mathbf{A}}_k^s = \text{diag}(\mathbf{a}_P(\phi_k) e^{j\pi P\phi_k \mathbf{p}(K_d)})$ and $\mathbf{d}_{k,m} = e^{j\pi\beta_{k,m}\mathbf{p}(K_d)}$, the beamforming vector $\mathbf{f}_{k,m} = \bar{\mathbf{A}}_k^s \mathbf{d}_{k,m}$ can achieve near-optimal array gain at frequency f_m on physical direction $\bar{\theta}_{k,m}$ as

$$\bar{\theta}_{k,m} = \frac{\phi_k}{\xi_m} + \frac{\beta_{k,m}}{\xi_m P}, \quad (9)$$

where $\beta_{k,m} \in [-1, 1]$ denotes the frequency-dependent phase shifts and $P = N/K_d$.

Proof: See **Lemma 2** in [3]. By transforming the physical direction ϕ_k to its spatial direction at the m -th subcarrier $\frac{\phi_k}{\xi_m}$, (9) can be easily proved by **Lemma 2** in [3]. ■

Considering the form of \mathbf{A}_k^s and \mathbf{t}_k , we can rewrite $\mathbf{f}_{k,m}$ as

$$\mathbf{f}_{k,m} = \text{diag}(\mathbf{a}_P(\phi_k) e^{j\pi P\phi_k \mathbf{p}(K_d)}) e^{j\pi(2s_k - 2\xi_m s_k)\mathbf{p}(K_d)}, \quad (10)$$

where $\xi_m = \frac{f_m}{f_c}$ and $T_c = \frac{1}{f_c}$. By comparing the form of $\bar{\mathbf{A}}_k^s$, $\mathbf{d}_{k,m}$ in **Lemma 2** and (10), the frequency-dependent phase-shift $\beta_{k,m}$ in **Lemma 2** can be represented by the number of periods that delayed s_k as

$$\beta_{k,m} = 2(1 - \xi_m)s_k. \quad (11)$$

Substituting s_k , ϕ_k and (11) into (9), the physical direction $\bar{\theta}_{k,m}$ of the beam $\mathbf{f}_{k,m}$ can be presented as

$$\begin{aligned} \bar{\theta}_{k,m} &= \frac{\phi_k}{\xi_m} - \left(\frac{1}{\xi_m} - 1\right)\left(\phi_k + \frac{2\xi_M\xi_1\alpha_k}{\xi_M - \xi_1}\right) \\ &= \theta_k^{(0)} + (1 - \xi_1)\alpha_k + \frac{2\xi_M\xi_1(\xi_m - 1)}{\xi_m(\xi_M - \xi_1)}\alpha_k, \end{aligned} \quad (12)$$

which proves (8).

Obviously, we can observe from (12) that the physical directions $\bar{\theta}_{k,m}$ of $\mathbf{f}_{k,m}$ with $m = 1, 2, \dots, M$ increases as m becomes larger. When $m = M$, we have

$$\bar{\theta}_{k,M} = \theta_k^{(0)} + (1 - \xi_1)\alpha_k + \frac{2\xi_M\xi_1(\xi_M - 1)}{\xi_M(\xi_M - \xi_1)}\alpha_k \stackrel{(a)}{=} \theta_k^{(0)} + \alpha_k, \quad (13)$$

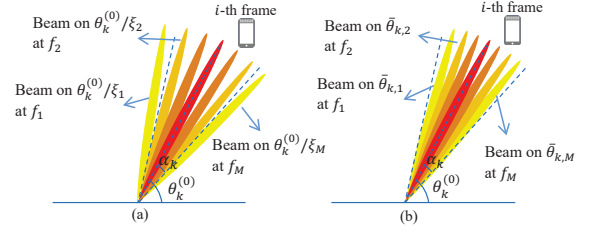


Fig. 4. BZ mechanism: (a) The beams without control by TDs; (b) The beams generated by DPP structure based on **Lemma 1**.

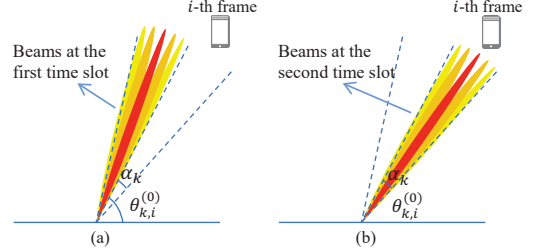


Fig. 5. The proposed BZ based beam tracking scheme with training overhead $T = 2$: (a) Beams generated at $t = 1$; (b) Beams generated at $t = 2$.

where (a) comes from $\xi_1 + \xi_M = 2$. Similar to (13), we can also obtain $\bar{\theta}_{k,1} = \theta_k^{(0)} - \alpha_k$. Therefore, considering $\bar{\theta}_{k,m}$ is monotonously increasing over m , the physical directions $\bar{\theta}_{k,m}$ with $m = 1, 2, \dots, M$ which the beam $\mathbf{f}_{k,m}$ is aligned with, can cover the tracking range $[\theta_k^{(0)} - \alpha_k, \theta_k^{(0)} + \alpha_k]$. ■

Lemma 1 illustrates that the angular coverage of beams is not fixed and determined by the beam split effect as shown in Fig. 4 (a), but can be flexibly controlled as shown in Fig. 4 (b). This BZ mechanism can be easily achieved by the delicate design of time delays in the DPP structure. Therefore, the BZ mechanism in **Lemma 1** can be utilized to generate beams tracking different physical directions at the same time.

C. Beam Zooming Based Beam Tracking Scheme

Based on the BZ mechanism discussed above, we propose a BZ based beam tracking scheme to realize fast beam tracking. The key idea of the proposed scheme is shown in Fig. 5. In each time slot, the angular coverage of frequency-dependent beams generated by DPP structure is flexibly zoomed to adapt the variation range of user physical direction, which means beams that cover a fraction of the required tracking range is generated. Then, multiple physical directions in this fraction of tracking range are tracked simultaneously. The above procedure is carried out T times over all T time slots until the whole tracking range is considered. Finally, the physical directions in the next frame can be obtained by maximizing the users received signal.

The procedure of the proposed BZ based beam tracking scheme is provided in **Algorithm 1**. Its target is to obtain the users physical directions $\theta_{k,i+1}^{(0)}$ at the $(i+1)$ -th frame based on the physical directions $\theta_{k,i}^{(0)}$ at the i -th frame. In step 1 and 2, the physical directions that will be tracked during the t -th time slot is calculated, where $\bar{\theta}_{k,i,\text{cen}}^{(t)}$ is the central physical direction of $[\theta_{k,i}^{(0)} - \alpha_k + \frac{(2t-2)\alpha_k}{T}, \theta_{k,i}^{(0)} - \alpha_k + \frac{2t\alpha_k}{T}]$ which is the t -th fraction of the tracking range, and $\bar{\theta}_{k,m,i}^{(t)}$ denotes the

physical direction that is tracked at the m -th subcarrier within the t -th time slot as

$$\bar{\theta}_{k,m,i}^{(t)} = \bar{\theta}_{k,i,\text{cen}}^{(t)} + (1 - \xi_1) \frac{\alpha_k}{T} + \frac{2\xi_M \xi_1 (\xi_m - 1)}{\xi_m (\xi_M - \xi_1) T} \alpha_k. \quad (14)$$

Then, all the physical directions that will be tracked during T time slots is combined as a targeted physical directions set Ψ_k^{i+1} in step 3.

After that, these physical directions are tracked during T time slots to guarantee the whole tracking range is considered. At the t -th time slot, beams that cover the t -th fraction of the tracking range $[\theta_{k,i}^{(0)} - \alpha_k + \frac{(2t-2)\alpha_k}{T}, \theta_{k,i}^{(0)} - \alpha_k + \frac{2t\alpha_k}{T}]$ is generated using the DPP structure in step 5 – 9, where the analog beamformer \mathbf{A}_m is calculated based on the parameters $\phi_k^{(t)}$ and $s_k^{(t)}$ proved in **Lemma 1** in step 5 as

$$\phi_k^{(t)} = \bar{\theta}_{k,i,\text{cen}}^{(t)} + (1 - \xi_1) \frac{\alpha_k}{T}, \quad (15)$$

$$s_k^{(t)} = -\frac{P}{2} \left(\phi_k^{(t)} + \frac{2\xi_M \xi_1 \alpha_k}{(\xi_M - \xi_1) T} \right). \quad (16)$$

Then, phase shifts provided by traditional PSs $\mathbf{A}_k^{s,(t)}$ and time delays provided by TDs $\mathbf{t}_k^{(t)}$ is designed in step 6 and 7. As proved in **Lemma 1**, when $\phi_k^{(t)}$ and $s_k^{(t)}$ satisfy (15) and (16), the beams generated as $\mathbf{f}_{k,m}^{(t)} = \mathbf{A}_k^{s,(t)} e^{-j2\pi f_m \mathbf{t}_k^{(t)}}$ is aligned with the physical direction $\bar{\theta}_{k,m,i}^{(t)}$, which is corresponding to the physical directions in Ψ_k^{i+1} generated in step 1 – 3. This makes the t -th fraction of tracking range is sufficiently covered. Based on $\mathbf{A}_k^{s,(t)}$ and $\mathbf{t}_k^{(t)}$, the analog beamformer at the t -th time slot $\mathbf{A}_m^{(t)}$ is calculated in step 8 and 9.

After the analog beamformer is calculated, the BS transmits training pilot sequence $\mathbf{q}_{k,m}^{(t)} \in \mathcal{C}^{Q \times 1}$ over total Q instants within the t -th time slot interval using the beamformer $\mathbf{A}_m^{(t)}$ at the m -th subcarrier. As shown in step 10, the received signal $\mathbf{Y}_{m,t} \in \mathcal{C}^{K \times Q}$ for K users is

$$\mathbf{Y}_{m,t} = \mathbf{H}_m^H \mathbf{A}_m^{(t)} \mathbf{Q}_m^{(t)} + \mathbf{N}^{(t)}, \quad (17)$$

where $\mathbf{Q}_m^{(t)} = [\mathbf{q}_{1,m}^{(t)}, \mathbf{q}_{2,m}^{(t)}, \dots, \mathbf{q}_{K,m}^{(t)}]^T$ denotes the pilot sequences of all K users. Based on the received signal, the user can calculate the label of the optimal beam t_k and m_k in step 12 by maximizing the received signal power as

$$(t_k, m_k) = \underset{t \in 1, 2, \dots, T, m \in 1, 2, \dots, M}{\arg \max} \|\mathbf{Y}_{m,t,[k,:]} \|_2^2. \quad (18)$$

Finally, the BS can obtain the physical directions $\theta_{k,i+1}^{(0)}$ through the feedback of t_k and m_k in step 13.

Two points about **Algorithm 1** should be emphasized: (1) The beam tracking procedures of different users are not separated, but simultaneously carried out in **Algorithm 1**, i.e., for the t -th time slot, $\mathbf{A}_m^{(t)}$ generates required beams for all the users as shown in step 9; (2) The pilot sequence $\mathbf{q}_{k,m}^{(t)}$ for the k -th user is generated as $[\mathbf{q}_{1,m}^{(t)}, \mathbf{q}_{2,m}^{(t)}, \dots, \mathbf{q}_{K,m}^{(t)}]^T = \mathbf{D}_m^{(t)} \mathbf{s}$, where the digital precoder $\mathbf{D}_m^{(t)}$ can be designed according to the required pilots $\mathbf{q}_{k,m}^{(t)}$, e.g., all elements in $\mathbf{q}_{k,m}^{(t)}$ are 1.

The advantage of the proposed BZ based beam tracking

scheme mainly reflects in two aspects. On one hand, the proposed scheme can generate beams aligned with different physical directions simultaneously, which is achieved by the flexible control of the angular coverage of beams generated by DPP structure, i.e., the degree of beam split effect. Therefore, it can reduce the training overhead T significantly, compared with the traditional beam tracking scheme which only tracks one physical direction in a single time slot. On the other hand, with the same training overhead T , the proposed BZ scheme is able to track M times the number of physical directions as much as the traditional beam tracking scheme. This increase of sample interval on angle domain improves the beam tracking accuracy of $\theta_{k,i+1}^{(0)}$.

Algorithm 1 Proposed BZ based beam tracking scheme.

Inputs:

Physical directions $\theta_{k,i}^{(0)}$; Range of user mobility α_k ; Beam tracking time slots T ; The number of the pilots in each time slot Q ; The number of TDs in a RF chain group K_d

Output:

Physical directions $\theta_{k,i+1}^{(0)}$

- 1: $\bar{\theta}_{k,i,\text{cen}}^{(t)} = \theta_{k,i}^{(0)} - \alpha_k + \frac{(2t-1)\alpha_k}{T}$
- 2: $\bar{\theta}_{k,m,i}^{(t)} = \bar{\theta}_{k,i,\text{cen}}^{(t)} + (1 - \xi_1) \frac{\alpha_k}{T} + \frac{2\xi_M \xi_1 (\xi_m - 1)}{\xi_m (\xi_M - \xi_1) T} \alpha_k$
- 3: $\Psi_k^{i+1} = [\bar{\theta}_{k,1,i}^{(1)}, \bar{\theta}_{k,2,i}^{(1)}, \dots, \bar{\theta}_{k,M,i}^{(1)}, \bar{\theta}_{k,1,i}^{(2)}, \bar{\theta}_{k,2,i}^{(2)}, \dots, \bar{\theta}_{k,M,i}^{(T)}]$
- 4: **for** $t \in \{1, 2, \dots, T\}$ **do**
- 5: $\phi_k^{(t)} = \bar{\theta}_{k,i,\text{cen}}^{(t)} + \frac{(1-\xi_1)\alpha_k}{T}$, $s_k^{(t)} = -\frac{P}{2} \left(\phi_k^{(t)} + \frac{2\xi_M \xi_1 \alpha_k}{(\xi_M - \xi_1) T} \right)$
- 6: $\mathbf{A}_k^{s,(t)} = \text{diag} \left(\mathbf{a}_P(\phi_k^{(t)}) e^{j\pi(P\phi_k^{(t)} + 2s_k^{(t)})} \mathbf{p}(K_d) \right)$
- 7: $\mathbf{t}_k = s_k^{(t)} T_c \mathbf{p}(K_d)$;
- 8: $\mathbf{f}_{k,m}^{(t)} = \mathbf{A}_k^{s,(t)} e^{-j2\pi f_m \mathbf{t}_k^{(t)}}$
- 9: $\mathbf{A}_m^{(t)} = [\mathbf{f}_{1,m}^{(t)}, \mathbf{f}_{2,m}^{(t)}, \dots, \mathbf{f}_{K,m}^{(t)}]$
- 10: $\mathbf{Y}_{m,t} = \mathbf{H}_m^H \mathbf{A}_m^{(t)} \mathbf{Q}_m^{(t)} + \mathbf{N}^{(t)}$
- 11: **end for**
- 12: $(t_k, m_k) = \underset{t \in 1, 2, \dots, T, m \in 1, 2, \dots, M}{\arg \max} \|\mathbf{Y}_{m,t,[k,:]} \|_2^2$
- 13: $\theta_{k,i+1}^{(0)} = \Psi_{k,[(t_k-1)M+m_k]}^{t+1}$
- 14: **return** $\theta_{k,i+1}^{(0)}$.

IV. SIMULATION RESULTS

In this section, several simulation results are provided to verify the performance of our proposed scheme. The parameters are set as: $N = 256$, $M = 128$, $K = 4$, $K_d = 16$, $f_c = 100$ GHz, $B = 10$ GHz, $L = 1$ and $Q = 10$. $\theta_{k,i}^{(0)}$ follows uniform distribution $\mathcal{U}(-1, 1)$, and α_k follows $\mathcal{U}(0, \alpha_{k,\text{max}})$. We assume the equivalent channel can be perfectly estimated. During data transmission, \mathbf{A}_m is designed based on (5) and (6), and \mathbf{D}_m is designed by zero-forcing (ZF) precoding. The achievable sum-rate performance is calculated using $R = \sum_1^K \sum_1^M \log_2(1 + \zeta_{k,m})$ and $\zeta_{k,m} = \frac{|\mathbf{h}_k^H \mathbf{A}_m \mathbf{D}_{m,[k,k]}|^2}{\sum_{k' \neq k} |\mathbf{h}_k^H \mathbf{A}_m \mathbf{D}_{m,[k,k']}|^2 + \sigma^2}$, and the signal-to-noise ratio (SNR) is defined as $\frac{\rho}{\sigma^2}$.

Fig. 6 shows the tracking accuracy of our proposed BZ based scheme, where the beam tracking results of four users

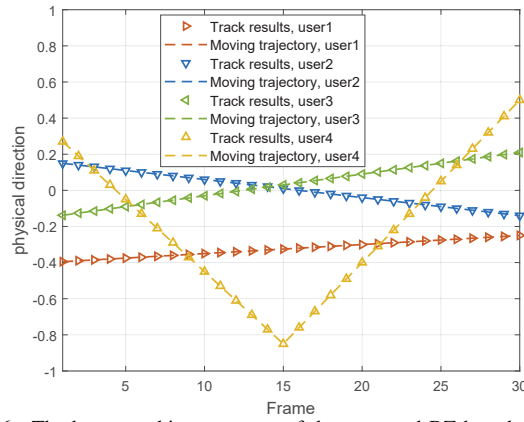


Fig. 6. The beam tracking accuracy of the proposed BZ based scheme.

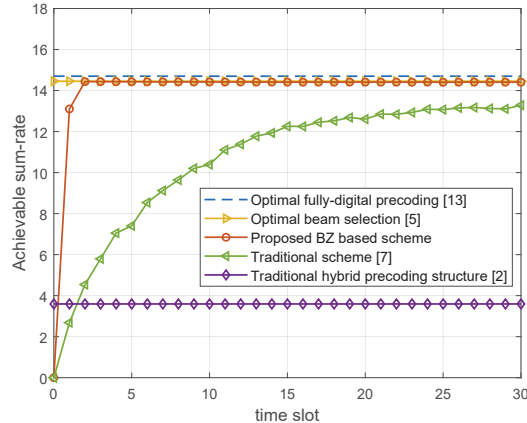


Fig. 7. Achievable sum-rate performance against the number of time slots T .

during 30 consecutive frames are shown with SNR = 10 dB, $\alpha_k = 0.1$ and $T = 5$. The initial physical direction $\theta_{k,0}^{(0)}$ and the moving velocity $\Delta_k = \theta_{k,i+1}^{(0)} - \theta_{k,i}^{(0)}$ of the users are set as $[\theta_{1,0}^{(0)}, \theta_{2,0}^{(0)}, \theta_{3,0}^{(0)}, \theta_{4,0}^{(0)}] = [-0.4, 0.16, -0.15, 0.35]$, $[\Delta_1, \Delta_2, \Delta_3] = [0.005, -0.01, 0.012]$, and $\Delta_4 = -0.08$ for $i < 15$, and $\Delta_4 = 0.08$ for $i \geq 15$. We can observe from Fig. 6 that our proposed scheme can correctly track the user trajectory. The deviation between the actual physical directions and the tracked results can be ignored, even for the user 4 who changes its motion direction during the tracking period.

In Fig. 7, we provide the achievable sum-rate performance against the number of beam tracking time slots T with $\alpha_{k,\max} = 0.1$, where the optimal fully digital ZF precoding [13], beam selection [5] with perfect physical directions, beam selection based on physical directions tracked by the proposed BZ based scheme, and beam selection based on the physical directions tracked by traditional beam tracking scheme [7] as described in III-A are provided using DPP structure. Additionally, beam selection with perfect physical directions using traditional hybrid precoding structure [2] is also illustrated. We can observe from Fig. 7 that by exploiting the proposed BZ based beam tracking scheme, the beam selection can achieve near-optimal achievable sum-rate performance with low training overhead, e.g., when $T > 2$, 98% optimal achievable sum-rate can be achieved. Moreover, the proposed BZ based scheme outperforms the traditional

beam tracking scheme with a nearly 95% training overhead reduction. Besides, due to the beam split effect, the beam selection with perfect physical directions under traditional hybrid precoding suffers from nearly 80% achievable sum-rate loss, which verifies the effectiveness of DPP structure in wideband THz massive MIMO.

V. CONCLUSIONS

In this paper, we solve the wideband beam tracking problem in THz massive MIMO systems based on the recently proposed DPP structure. A BZ based beam tracking scheme is proposed, where multiple physical directions are tracked simultaneously using beams generated by the DPP structure. The coverage of these beams is flexibly adjusted to cover the potential range of user motion. Simulation results verify that the proposed BZ based scheme can reduce training overhead by 95%, and achieve nearly 98% of the optimal achievable sum-rate.

ACKNOWLEDGMENTS

This work was supported by the National Science and Technology Major Project of China under Grant 2018ZX03001004-003 and the National Natural Science Foundation of China for Outstanding Young Scholars under Grant 61722109.

REFERENCES

- [1] B. Peng, K. Guan, and T. Kurner, "Cooperative dynamic angle of arrival estimation considering space time correlations for terahertz communications," *IEEE Trans. Wireless Commun.*, vol. 17, no. 9, pp. 6029–6041, Sep. 2018.
- [2] O. E. Ayach, S. Rajagopal, S. Abu-Surra, Z. Pi, and R. W. Heath, "Spatially sparse precoding in millimeter wave MIMO systems," *IEEE Trans. Wireless Commun.*, vol. 13, no. 3, pp. 1499–1513, Mar. 2014.
- [3] J. Tan and L. Dai, "Delay-phase precoding for THz massive MIMO with beam split," in *Proc. IEEE Global Commun. Conf. (IEEE GLOBECOM'19)*, Dec. 2019, pp. 1–6.
- [4] R. Piesiewicz, T. Kleine-Ostmann, N. Krumbholz, D. Mittleman, M. Koch, J. Schoebel, and T. Kurner, "Short-range ultra-broadband terahertz communications: Concepts and perspectives," *IEEE Antennas Propag. Mag.*, vol. 49, no. 6, pp. 24–39, Dec. 2007.
- [5] A. Ali, N. Gonzalez-Prelcic, and R. W. Heath, "Millimeter wave beam-selection using out-of-band spatial information," *IEEE Trans. Wireless Commun.*, vol. 17, no. 2, pp. 1038–1052, Feb. 2018.
- [6] X. Rao and V. K. N. Lau, "Distributed compressive CSIT estimation and feedback for FDD multi-user massive MIMO systems," *IEEE Tran. Signal Process.*, vol. 62, no. 12, pp. 3261–3271, Jun. 2014.
- [7] IEEE, "IEEE802.11-10/0433r2, PHY/MAC complete proposal specification (TGad D0.1)," 2010.
- [8] S. Hur, T. Kim, D. J. Love, J. V. Krogmeier, T. A. Thomas, and A. Ghosh, "Millimeter wave beamforming for wireless backhaul and access in small cell networks," *IEEE Trans. Commun.*, vol. 61, no. 10, pp. 4391–4403, Oct. 2013.
- [9] D. Zhu, J. Choi, Q. Cheng, W. Xiao, and R. W. Heath, "High-resolution angle tracking for mobile wideband millimeter-wave systems with antenna array calibration," *IEEE Trans. Wireless Commun.*, vol. 17, no. 11, pp. 7173–7189, Nov. 2018.
- [10] L. You, X. Gao, G. Y. Li, X. Xia, and N. Ma, "BDMA for millimeter-wave/terahertz massive MIMO transmission with per-beam synchronization," *IEEE J. Sel. Areas Commun.*, vol. 35, no. 7, pp. 1550–1563, Jul. 2017.
- [11] R. W. Heath, N. Gonzalez-Prelcic, S. Rangan, W. Roh, and A. M. Sayeed, "An overview of signal processing techniques for millimeter wave MIMO systems," *IEEE J. Sel. Top. Signal Process.*, vol. 10, no. 3, pp. 436–453, Apr. 2016.
- [12] C. Wang, L. Ma, R. Li, T. S. Durrani, and H. Zhang, "Exploring trajectory prediction through machine learning methods," *IEEE Access*, vol. 7, pp. 101 441–101 452, Jul. 2019.
- [13] D. Tse and P. Viswanath, *Fundamentals of Wireless Communication*. Cambridge, U.K.: Cambridge Univ. Press, 2005.